11^{th} International Conference on Fracture Mechanics of Concrete and Concrete Structures
FraMCoS-11
J. M. Chandra Kishen, A. Ramaswamy, S. Ray and R. Vidyasagar (Eds)
https://doi.org/10.21012/FC11.092392

MICROMECHANICS-BASED PHASE-FIELD MODELING OF FATIGUE IN (QUASI-)BRITTLE MATERIALS

MINA SAREM*, NUHAMIN E. DERESSE*, JACINTO ULLOA†, ELS VERSTRYNGE* AND STIJN FRANÇOIS*

*KU Leuven
Leuven, Belgium
e-mail: mina.sarem@kuleuven.be

†California Institute of Technology
Pasadena, CA USA

Key words: (Quasi-)brittle Materials, Micromechanics-based Phase-field Models, Fatigue Failure, Cyclic Loading

Abstract. This paper presents an extended micromechanics-based phase-field variational model for fatigue fracture. The approach involves incorporating a fatigue degradation function to contribute to a reduction in fracture toughness, driven by free energy accumulation. The model's performance is evaluated through the application of cyclic loading on a single volume element. This study investigates the influence of fatigue parameters on the model's behavior and outcomes.

1 INTRODUCTION

Fatigue failure in (quasi-)brittle materials such as concrete is an important design aspect of structures and materials. Fatigue can occur due to repeated loading and unloading cycles, leading to microcrack initiation and propagation, ultimately resulting in failure. The understanding of fatigue behavior is challenging because of the complex interplay between microstructure, fatigue damage mechanisms, and loading conditions.

Predicting fatigue behavior in (quasi-)brittle materials has been challenging and remained a captivating subject. Many studies have investigated fatigue phenomenon, employing different numerical methodologies and phenomenological formulations to simulate this behavior. Among these methods, phase-field approach for modeling fracture in (quasi-)brittle materials like mortar and concrete has gained significant attention in recent years for its ability to capture arbitrarily complicated crack paths, including crack initiation, propagation and branching [1]. However, it has some limitations, such as the inability to distinguish between tensile and compressive failure, which can lead to the development of unrealistic crack patterns in compression [2]. To address these limitations, various modifications have been proposed for the phase-field approach, such as the one suggested by Amor et al. [3] to decompose the elastic energy density into its volumetric and deviatoric parts and to degrade only the volumetric contribution, thus avoiding cracking under compression and preventing the interpenetration of crack faces [1]. Another modification, proposed by Miehe et al. [4], involves using a spectral split, which decomposes the strain tensor to degrade only the tensile energy. However, these modifications are heuristic in nature and may lack physical insight, making it challenging to understand the underlying physics of the system

being modeled.

Another method that introduces a way to differentiate between failure modes is the micromechanics-based phase-field model, such as the model proposed by Ulloa et al. [5] or the one proposed by You et al. [6]. These models represent an advancement in the phase-field modeling by containing multiple crack modes for which the split comes in naturally from the model and makes the computations more robust. The micromechanical models of isotropic damage in brittle materials consider damaged materials as heterogeneous media composed of solid matrix weakened by isotropically distributed microcracks. These models provide a proper micromechanical thermodynamic formulation for damage-friction modeling in brittle materials with the help of Eshelby's solution to matrix-inclusion problems. The damage evolution law is formulated in a sound thermodynamic framework and inherently coupled with frictional sliding [7].

The micromechanics-based phase-field model aims to connect field variables at the macroscale with physical dissipative mechanisms at the microcrack level. The model distinguishes between close and open microcracks to capture different fracture modes naturally, without implementing heuristic energy decompositions.

Therefore, the present study focuses on the use of micromechanics-based phase-field modeling to simulate the fatigue behavior. Many researchers have explored the incorporation of fatigue phenomenon in phase-field modeling in recent years [8, 9]. To account for fatigue and cyclic effects, several degraded functions have been suggested to reduce fracture toughness. For example, Alessi et al. [10] introduced a function that decreases fracture energy as strain increases. In this context, the present study adopts the model proposed by Carrara et al. [11], where they utilized degraded free energy density as a history variable, which accumulates over loading cycles once a specific threshold is surpassed.

This paper is organized as follows. The main ingredients of the adopted micromechanics-based phase-field model is presented in section 2. These concepts are used to construct the fatigue model in section 3. The numerical example is illustrated in section 4. Finally, section 5 presents the conclusions of the work.

2 MICROMECHANICS-BASED PHASE-FIELD MODEL

In this section, the micromechanics-based phase-field model proposed by Ulloa et al. [5] is briefly recalled. This model considers a matrix-inclusion system with penny-shaped microcracks inside a representative volume element (RVE). Moreover, the microcracks are assumed to be uniformly distributed in all directions and result in an isotropic behavior of the RVE. For more details, the reader is referred to [5, 6].

In micromechanics-based models, dissipation phenomena at macro-scale like damage and plasticity can be explained by the existence of microcracks in the material on a lower scale [7, 12,13]. Frictional sliding of microcracks caused by compression/shear results in the occurrence of irreversible strains which is interpreted as plasticity at the macro-scale. Accordingly, damage can be explained by the localization and growth of microcracks which leads to the loss of stiffness at the macro level [14].

The state of the solid can be defined by three field variables: the displacement field $u\colon \Omega \times \mathrm{T} \to \mathbb{R}^3$, the crack phase-field $\alpha\colon \Omega \times \mathrm{T} \to [0,1]$ and the plastic strain tensor $\varepsilon^{\mathrm{p}}\colon \Omega \times \mathrm{T} \to \mathbb{R}^{3\times3}_{\mathrm{sym}}$. In the classical phase-field approach, the degradation function multiplies the elasticity tensor to reduce the energy during damage. However, this is not realistic since it gives a symmetric behavior in tension and compression. To address this problem, the asymmetric behavior is naturally incorporated in micromechanics-based model formulation by distinguishing between open and closed microcracks, designated as open and closed in this study. The micromechanics-based phase-field model is summarized in tables 1 and 2 (adopted from [5]).

Table 1: Energy quantities and state equations.

Free energy and state equations	
Stored energy	$\psi(\boldsymbol{\varepsilon},\boldsymbol{\varepsilon}^{\mathrm{p}},\alpha)=\begin{cases}\frac{1}{2}\boldsymbol{\varepsilon}:\mathbf{C}^{\mathrm{dam}}(\alpha):\boldsymbol{\varepsilon} & \text{if open,}\\ \frac{1}{2}(\boldsymbol{\varepsilon}-\boldsymbol{\varepsilon}^{\mathrm{p}}):\mathbf{C}:(\boldsymbol{\varepsilon}-\boldsymbol{\varepsilon}^{\mathrm{p}})+\frac{1}{2}\boldsymbol{\varepsilon}^{\mathrm{p}}:\mathbf{H}^{\mathrm{kin}}(\alpha):\boldsymbol{\varepsilon}^{\mathrm{p}} & \text{if closed}\end{cases}$
Generalized stresses	$\boldsymbol{\sigma}(\boldsymbol{\varepsilon},\boldsymbol{\varepsilon}^{\mathrm{p}},\alpha)=\dfrac{\partial\psi}{\partial\boldsymbol{\varepsilon}},\quad s^{\mathrm{p}}(\boldsymbol{\varepsilon},\boldsymbol{\varepsilon}^{\mathrm{p}},\alpha)=-\dfrac{\partial\psi}{\partial\boldsymbol{\varepsilon}^{\mathrm{p}}},\quad s^{\mathrm{d}}(\boldsymbol{\varepsilon},\boldsymbol{\varepsilon}^{\mathrm{p}},\alpha)=-\dfrac{\partial\psi}{\partial\alpha}$
Opening/closure transition	$\begin{cases}\operatorname{tr} s^{\mathrm{p}}(\boldsymbol{\varepsilon},\boldsymbol{\varepsilon}^{\mathrm{p}},\alpha)=0 & \text{if open,}\\ \operatorname{tr} s^{\mathrm{p}}(\boldsymbol{\varepsilon},\boldsymbol{\varepsilon}^{\mathrm{p}},\alpha)<0 & \text{if closed}\end{cases}$
Dissipation potential: $\phi=\phi^{\mathrm{p}}+\phi^{\mathrm{d}}\geq 0$	
Plastic dissipation potential	$\phi^{\mathrm{p}}(\dot{\boldsymbol{\varepsilon}}^{\mathrm{p}};s^{\mathrm{p}})=\begin{cases}\dfrac{\operatorname{tr}\dot{\boldsymbol{\varepsilon}}^{\mathrm{p}}}{3A_\theta}(A_\theta-A_\varphi)\operatorname{tr} s^{\mathrm{p}} & \text{if } \operatorname{tr}\dot{\boldsymbol{\varepsilon}}^{\mathrm{p}}\geq\sqrt{6}A_\theta\|\dot{\boldsymbol{\varepsilon}}^{\mathrm{p}}_{\mathrm{dev}}\|,\\ +\infty & \text{otherwise}\end{cases}$
Damage dissipation potential	$\phi^{\mathrm{d}}(\dot\alpha,\nabla\dot\alpha;\alpha,\nabla\alpha,\boldsymbol{s}^{\mathrm{p}})=\begin{cases}\dfrac{G_{\mathrm{c}}(\boldsymbol{s}^{\mathrm{p}})}{\ell}\big(\alpha\,\dot\alpha+\ell^2\nabla\alpha\cdot\nabla\dot\alpha\big) & \text{if } \dot\alpha\geq 0,\\ +\infty & \text{otherwise}\end{cases}$

3 EXTENSION TO FATIGUE BEHAVIOR

In this section, the micromechanics-based phase-field approach is extended to address fatigue phenomenon. Similar to [11, 15], fatigue effects are considered employing a fatigue variable γ and a fatigue degradation function $d(\gamma)$ with the following properties

$$d(\gamma\leq\gamma_0)=1,\quad d(\gamma>\gamma_0)\in[0,1],\quad d'(\gamma)\leq 0, \tag{1}$$

in which γ_0 is a material threshold parameter.

The dissipation potential reads

$$\phi(\dot{\boldsymbol{\varepsilon}}^{\mathrm{p}},\dot\alpha,\nabla\dot\alpha;\alpha,\nabla\alpha,\boldsymbol{s}^{\mathrm{p}})=\phi^{\mathrm{p}}(\dot{\boldsymbol{\varepsilon}}^{\mathrm{p}};\boldsymbol{s}^{\mathrm{p}})+\phi^{\mathrm{d}}(\dot\alpha,\nabla\dot\alpha;\alpha,\nabla\alpha,\boldsymbol{s}^{\mathrm{p}}), \tag{2}$$

where ϕ^{p} and ϕ^{d} are plastic and damage dissipation potentials. The plastic dissipation potential remains unchanged and is given by

$$\phi^{\mathrm{p}}(\dot{\boldsymbol{\varepsilon}}^{\mathrm{p}};s^{\mathrm{p}})=\begin{cases}\dfrac{\operatorname{tr}\dot{\boldsymbol{\varepsilon}}^{\mathrm{p}}}{3A_\theta}(A_\theta-A_\varphi)\operatorname{tr} s^{\mathrm{p}}\\ \qquad\qquad\text{if } \operatorname{tr}\dot{\boldsymbol{\varepsilon}}^{\mathrm{p}}\geq\sqrt{6}A_\theta\|\dot{\boldsymbol{\varepsilon}}^{\mathrm{p}}_{\mathrm{dev}}\|,\\ +\infty\quad\text{otherwise,}\end{cases} \tag{3}$$

while the damage dissipation potential is modified following [10, 11] as shown below

$$\phi^{\mathrm{d}}(\dot\alpha,\nabla\dot\alpha;\alpha,\nabla\alpha,\boldsymbol{s}^{\mathrm{p}})=\begin{cases}d(\gamma)\dfrac{G_{\mathrm{c}}(\boldsymbol{s}^{\mathrm{p}})}{\ell}\big(\alpha\,\dot\alpha+\ell^2\nabla\alpha\cdot\nabla\dot\alpha\big)\\ \qquad\qquad\text{if } \dot\alpha\geq 0,\\ +\infty\quad\text{otherwise.}\end{cases} \tag{4}$$

The fatigue degradation function serves as a tuning parameter for dissipation, impacting both the local and gradient phase-field components. Consequently, it maintains the same characteristics of the micromechanics-based phase-field model as in the monotonic case. This implies that dissipation remains exclusively related to the damage variable [11].

The choice of the degradation function is arbitrary. In the literature, researchers have proposed to degrade the fracture energy as the material mileage in terms of strain, stress or energy, increases. In this study, the fatigue history variable is formulated to depend on both elastic and plastic free energies, aligning with the concept of fracture and energy minimization. We incorporated two categories of fatigue degradation functions—namely, asymptotic and logarithmic—to effectively characterize the fatigue-induced damage. The asymptotic degradation

Table 2: Governing equations according to the energetic formulation.

Kinematic admissibility	
Infinitesimal strain	$\varepsilon(u) = \nabla^{\mathrm{s}} u$
Dirichlet boundary condition	$u = \bar{u} \ \text{ on } \Gamma_{\mathrm{D}}$
Mechanical balance	
Stress	$\sigma(\boldsymbol{\varepsilon}, \boldsymbol{\varepsilon}^{\mathrm{p}}, \alpha) = \begin{cases} \mathbf{C}^{\mathrm{dam}}(\alpha) : \boldsymbol{\varepsilon} & \text{if } \operatorname{tr} s^{\mathrm{p}}(\boldsymbol{\varepsilon}, \boldsymbol{\varepsilon}^{\mathrm{p}}, \alpha) = 0 \quad (\mathsf{open}), \\ \mathbf{C} : (\boldsymbol{\varepsilon} - \boldsymbol{\varepsilon}^{\mathrm{p}}) & \text{if } \operatorname{tr} s^{\mathrm{p}}(\boldsymbol{\varepsilon}, \boldsymbol{\varepsilon}^{\mathrm{p}}, \alpha) < 0 \quad (\mathsf{closed}) \end{cases}$
Equilibrium	$\operatorname{div} \boldsymbol{\sigma}(\boldsymbol{\varepsilon}, \boldsymbol{\varepsilon}^{\mathrm{p}}, \alpha) + \rho \boldsymbol{b} = \mathbf{0} \ \text{ in } \Omega$
Neumann boundary condition	$\boldsymbol{\sigma}(\boldsymbol{\varepsilon}, \boldsymbol{\varepsilon}^{\mathrm{p}}, \alpha) \cdot \boldsymbol{n} = \bar{\boldsymbol{t}} \ \text{ on } \Gamma_{\mathrm{N}}$
Plastic evolution problem	
Generalized stress	$s^{\mathrm{p}}(\boldsymbol{\varepsilon}, \boldsymbol{\varepsilon}^{\mathrm{p}}, \alpha) = \mathbf{C} : (\boldsymbol{\varepsilon} - \boldsymbol{\varepsilon}^{\mathrm{p}}) - \mathbf{H}^{\mathrm{kin}}(\alpha) : \boldsymbol{\varepsilon}^{\mathrm{p}}$
Yield function	$f^{\mathrm{p}}(\boldsymbol{s}^{\mathrm{p}}) = \lVert s^{\mathrm{p}}_{\mathrm{dev}} \rVert + \sqrt{2/3}\, A_\varphi \operatorname{tr} s^{\mathrm{p}}$
Plastic potential	$g^{\mathrm{p}}(\boldsymbol{s}^{\mathrm{p}}) = \lVert s^{\mathrm{p}}_{\mathrm{dev}} \rVert + \sqrt{2/3}\, A_\theta \operatorname{tr} s^{\mathrm{p}}$
KKT system	$f^{\mathrm{p}}(\boldsymbol{s}^{\mathrm{p}}) \le 0, \quad \lambda \ge 0, \quad \lambda\, f^{\mathrm{p}}(\boldsymbol{s}^{\mathrm{p}}) = 0 \ \text{ in } \Omega$
Flow rule	$\dot{\boldsymbol{\varepsilon}}^{\mathrm{vp}} = \lambda\, \hat{\boldsymbol{n}}, \quad \hat{\boldsymbol{n}} \in \partial g^{\mathrm{p}}(\boldsymbol{s}^{\mathrm{p}}) = \partial \lVert s^{\mathrm{p}}_{\mathrm{dev}} \rVert + \sqrt{2/3}\, A_\theta \mathbf{1} \ \text{ in } \Omega$
Damage evolution problem	
Generalized stress	$s^{\mathrm{d}}(\boldsymbol{\varepsilon}, \boldsymbol{\varepsilon}^{\mathrm{p}}, \alpha) = \begin{cases} -\frac{1}{2} \boldsymbol{\varepsilon} : \mathbf{C}^{\mathrm{dam}\prime}(\alpha) : \boldsymbol{\varepsilon} & \text{if } \operatorname{tr} s^{\mathrm{p}}(\boldsymbol{\varepsilon}, \boldsymbol{\varepsilon}^{\mathrm{p}}, \alpha) = 0 \quad (\mathsf{open}), \\ -\frac{1}{2} \boldsymbol{\varepsilon}^{\mathrm{p}} : \mathbf{H}^{\mathrm{kin}\prime}(\alpha) : \boldsymbol{\varepsilon}^{\mathrm{p}} & \text{if } \operatorname{tr} s^{\mathrm{p}}(\boldsymbol{\varepsilon}, \boldsymbol{\varepsilon}^{\mathrm{p}}, \alpha) < 0 \quad (\mathsf{closed}) \end{cases}$
Yield function	$f^{\mathrm{d}}(s^{\mathrm{d}}; s^{\mathrm{p}}) = s^{\mathrm{d}} - \dfrac{G_{\mathrm{c}}(s^{\mathrm{p}})}{\ell} \alpha + \ell \operatorname{div}[G_{\mathrm{c}}(s^{\mathrm{p}}) \nabla \alpha]$
KKT system	$f^{\mathrm{d}}(s^{\mathrm{d}}; s^{\mathrm{p}}) \le 0, \quad \dot{\alpha} \ge 0, \quad \dot{\alpha}\, f^{\mathrm{d}}(s^{\mathrm{d}}; s^{\mathrm{p}}) = 0 \ \text{ in } \Omega$
Boundary condition	$\nabla \alpha \cdot \boldsymbol{n} = 0 \ \text{ on } \Gamma$

function is given by

$$d(\gamma) \coloneqq \begin{cases} 1 & \text{if} \quad \gamma(\boldsymbol{x}, t) \le \gamma_0, \\ \left(\dfrac{2\gamma_0}{\gamma(\boldsymbol{x}, t) + \gamma_0} \right)^2 & \text{if} \quad \gamma(\boldsymbol{x}, t) \ge \gamma_0, \end{cases} \tag{5}$$

and the logarithmic degradation function is shown below

$$d(\gamma) \coloneqq \begin{cases} 1 & \text{if} \quad \gamma(\boldsymbol{x}, t) \le \gamma_0, \\ \left[1 - k \log \left(\dfrac{\gamma(\boldsymbol{x}, t)}{\gamma_0} \right) \right]^2 & \text{if} \quad \gamma_0 \le \gamma(\boldsymbol{x}, t) \le \gamma_0 10^{1/k}, \\ 0 & \text{if} \quad \gamma(\boldsymbol{x}, t) \ge \gamma_0, \end{cases} \tag{6}$$

where k is a material parameter tuning the slope of the logarithmic function. The fatigue variable γ can now be defined as

$$\gamma(\boldsymbol{x}, t) \coloneqq \int_0^t \dot{\vartheta}(\boldsymbol{x}, s) H(\dot{\vartheta}(\boldsymbol{x}, s))\, \mathrm{d}s,$$

$$\text{with} \quad \vartheta(\boldsymbol{x}, t) \coloneqq \begin{cases} \dfrac{1}{2} : \varepsilon : \mathsf{C}^{\mathrm{dam}}(\alpha) : \varepsilon & \text{if open}, \\ \dfrac{1}{2} : \varepsilon^{\mathrm{p}} : \mathsf{H}^{\mathrm{kin}}(\alpha) : \varepsilon^{\mathrm{p}} & \text{if close}, \end{cases} \tag{7}$$

in which H represents the Heaviside function, preventing fatigue degradation during unloading.

Furthermore, the damage yield function is modified as follows

$$f^{\mathrm{d}}(s^{\mathrm{d}}; s^{\mathrm{p}}) \coloneqq s^{\mathrm{d}} - d(\gamma) \frac{G_{\mathrm{c}}(s^{\mathrm{p}})}{\ell} \alpha + \ell \operatorname{div}[d(\gamma) G_{\mathrm{c}}(s^{\mathrm{p}}) \nabla \alpha]. \tag{8}$$

It is important to highlight that the remaining formulation will closely follow the explanation provided in [16], which is summarized in tables 1 and 2. In the subsequent section, the behavior of a single volume element under cyclic loading is analyzed and the impact of fatigue parameters within the model is explored.

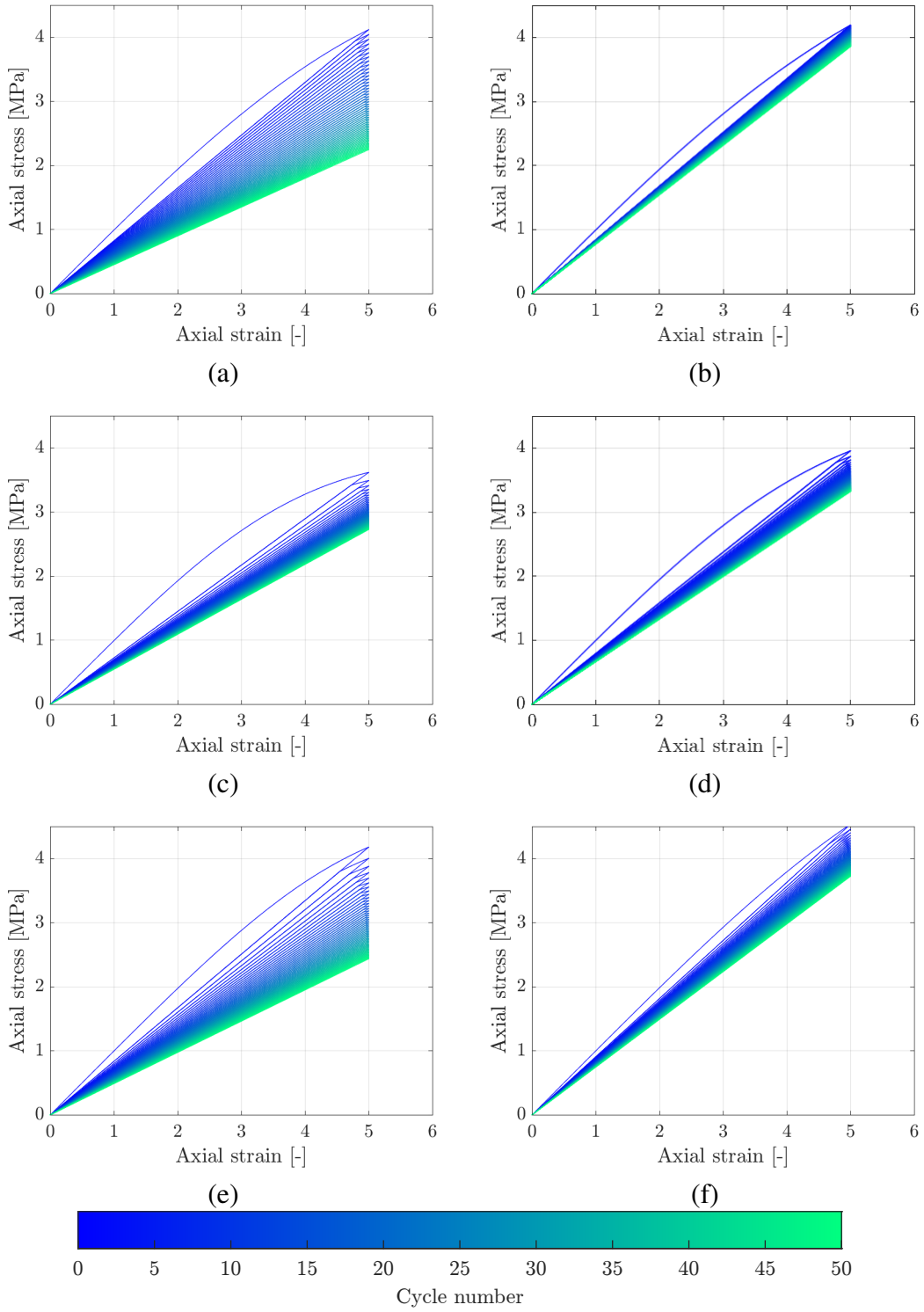

Figure 1: Axial stress vs. axial strain of the volume element with asymptotic degradation function for (a) and (b), and logarithmic degradation function for (c), (d), (e) and (f). (a), (c) and (e) are plotted for $\gamma_0 = 10$ and (b), (d) and (f) are drawn for $\gamma_0 = 100$. k is increased from 0.3 ((c) and (d)) to 0.8 ((e) and (f)).

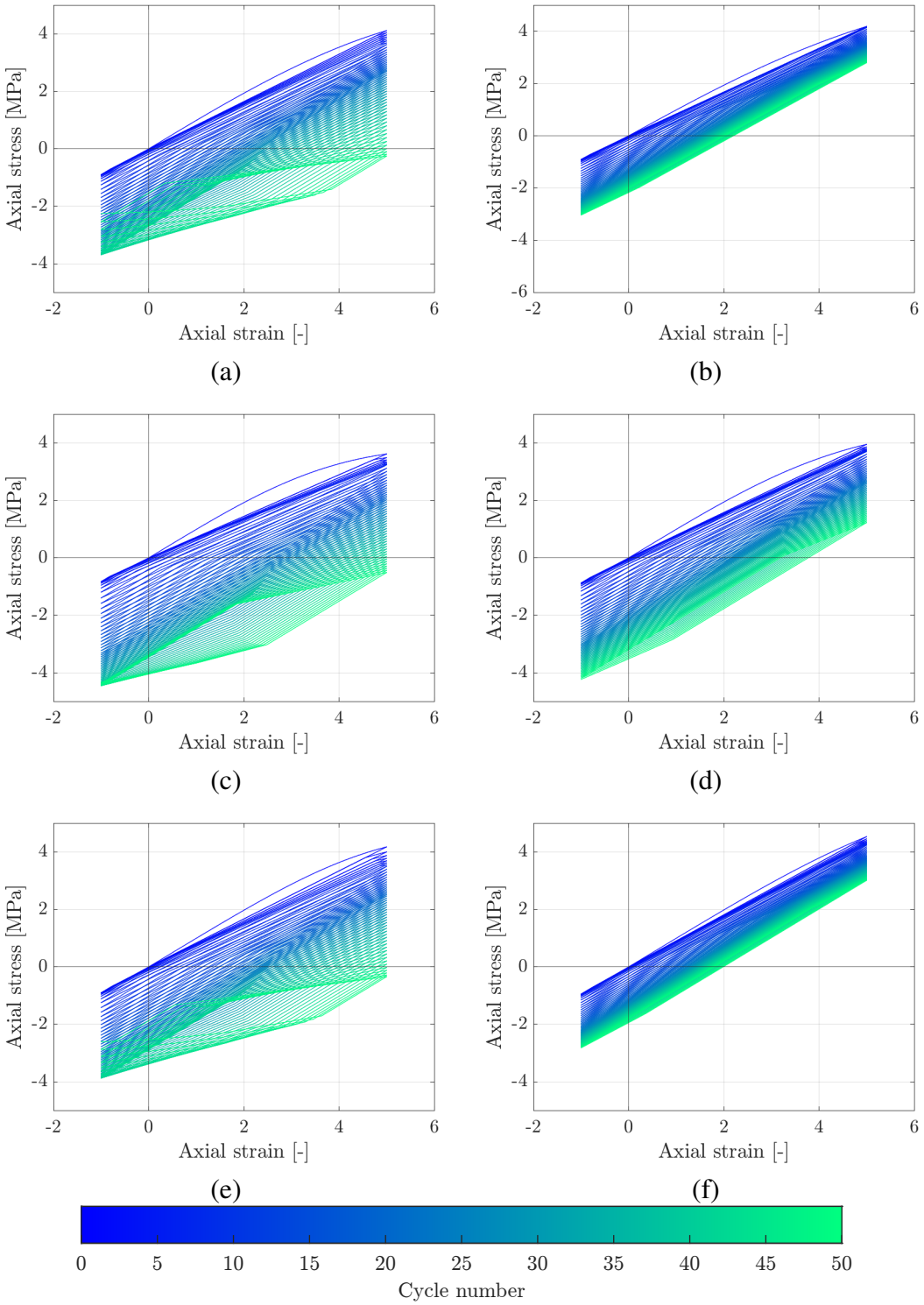

Figure 2: Axial stress vs. axial strain of the volume element with asymptotic degradation function for (a) and (b), and logarithmic degradation function for (c), (d), (e) and (f). (a), (c) and (e) are plotted for $\gamma_0 = 10$ and (b), (d) and (f) are drawn for $\gamma_0 = 100$. k is increased from 0.3 ((c) and (d)) to 0.8 ((e) and (f)).

4 NUMERICAL EXAMPLE: HOMOGENEOUS RESPONSE

To examine the influence of fatigue parameters on the model's behavior and the difference between the asymptotic and logarithmic degradation functions introduced earlier, the homogeneous response of a representative volume element (RVE) is analyzed. To this end, an RVE with the following material parameters is considered: Poisson's ratio $\nu = 0.2$, Young's modulus $E = 1$ MPa, degradation constant $b = 2$, initial damage $\alpha_0 = 1 \times 10^{-4}$, mode I fracture toughness $G_{\mathrm{cI}} = 5\frac{\mathrm{N}}{\mathrm{mm}}$, mode II fracture toughness $G_{\mathrm{cII}} = 50\frac{\mathrm{N}}{\mathrm{mm}}$ and friction and dilation coefficients $A_\varphi = 0.1$ and $A_\theta = 0.075$, respectively.

The volume element is first subjected to strain cycles ranging from 0 to 5, with axial strain incrementally applied in steps of 0.01. The relationship between axial strain and axial stress for the RVE with different fatigue parameters is depicted in Figure 1. In the next stage, the RVE experiences both tension and compression, with strain varying from -1 to 5. Both Figures 1 and 2 exhibit the same material properties, differing solely in the applied load between them. In order to enhance the visibility of fatigue-induced damage, low fatigue thresholds have been selected.

In Figures 1(or 2) (a) and (b), the asymptotic degradation function is employed, while Figures 1(or 2) (c), (d), (e), and (f) employ the logarithmic degradation function. The left-sided figures correspond to a fatigue threshold of $\gamma_0 = 30$, whereas the right-sided figures are generated for a higher fatigue threshold ($\gamma_0 = 100$). For the logarithmic degradation function, the impact of the parameter k is investigated by varying it from $k = 0.3$ in Figures 1(or 2) (c) and (d) to $k = 0.8$ in Figures 1(or 2) (e) and (f). In the case of the asymptotic degradation function the results in Figures 1(or 2) (a) and (b) demonstrate that an increase in γ_0 from 30 to 100 leads to a reduction in fatigue-induced degradation. A similar trend is observed for the logarithmic degradation function, as illustrated in Figure 1(or 2) (c), (d), (e) and (f). When comparing Figure 1(or 2) (c) to (e) and (d) to (f), it becomes evident that an increase in the parameter k amplifies the stress difference between the initial and final cycles. This parameter, k, can be understood as a tuning factor that enhances the model's adaptability during calibration against experimental data.

5 CONCLUSIONS

This research extends a micromechanics-based variational phase-field formulation to account for the influence of fatigue phenomenon in (quasi-)brittle materials subjected to cyclic loading. The fatigue damage mechanism is incorporated into the model by introducing a damage variable that evolves with fatigue loading cycles and diminishes the fracture toughness. The pace of reduction is controlled by a fatigue degradation function, solely dependent on the fatigue history variable. The damage variable is used to monitor the initiation and propagation of open microcracks, which ultimately lead to fatigue-induced failure.

The model is employed to simulate the fatigue response of a single volume element subjected to cyclic loading. The impact of fatigue parameters on the behavior of the volume element has been explored. The selection of both the fatigue history variable and the fatigue degradation function offers considerable flexibility. In this study, the fatigue history variable is defined as the accumulated active parts of the elastic and plastic strain energy densities. A comparison between two fatigue degradation functions (asymptotic and logarithmic) has been undertaken. Notably, the logarithmic fatigue degradation function provides more flexibility in calibrating the model to experimental data, enabling to attain the desired fatigue behavior.

The model offers insights into the micromechanical processes governing the fatigue behavior of materials and has the potential for extension to address boundary value problems in future studies.

REFERENCES

[1] Ambati, M. and Gerasimov, T. and De Lorenzis, L. 2015. A review on phase-field models of brittle fracture and a new fast hybrid formulation. *Computational Mechanics*, 55:383–405.

[2] Bourdin, B. and Francfort, G.A. and Marigo, J.J. 2000. Numerical experiments in revisited brittle fracture. *Journal of the Mechanics and Physics of Solids*, 48(4):797–826.

[3] Amor, H. and Marigo, J.J. and Maurini, C. 2009. Regularized formulation of the variational brittle fracture with unilateral contact: Numerical experiments. *Journal of the Mechanics and Physics of Solids*, 57(8):1209–1229.

[4] Miehe, C. and Hofacker, M. and Welschinger, F. 2010. A phase field model for rate-independent crack propagation: Robust algorithmic implementation based on operator splits. *Computer Methods in Applied Mechanics and Engineering*, 199(45-48):2765–2778.

[5] Ulloa, J. and Wambacq, J. and Alessi, R. and Samaniego, E. and Degrande, G. and Francois, S. 2022. A micromechanics-based variational phase-field model for fracture in geomaterials with brittle-tensile and compressive-ductile behavior. *Journal of the Mechanics and Physics of Solids*, 159:104684.

[6] You, T. and Waisman, H. and Chen, W.Z. and Shao, J.F. and Zhu, Q.Z. 2021. A novel micromechanics-enhanced phase-field model for frictional damage and fracture of quasi-brittle geomaterials. *Computer Methods in Applied Mechanics and Engineering*, 385:114060.

[7] Zhu, Q.Z. and Kondo, D. and Shao, J.F. 2008. Micromechanical analysis of coupling between anisotropic damage and friction in quasi brittle materials: role of the homogenization scheme. *International Journal of Solids and Structures*, 45(5):1385–1405.

[8] Khalil, Z. and Elghazouli, A.Y. and Martinez-Paneda, E. 2022. A generalised phase field model for fatigue crack growth in elastic–plastic solids with an efficient monolithic solver. *Computer Methods in Applied Mechanics and Engineering*, 388:114286.

[9] Schröder, J and Pise, M and Brands, D and Gebuhr, G and Anders, S. 2022. Phase-field modeling of fracture in high performance concrete during low-cycle fatigue: Numerical calibration and experimental validation. *Computer Methods in Applied Mechanics and Engineering*, 398:115181.

[10] Alessi, R. and Vidoli, S. and De Lorenzis, L. 2018. A phenomenological approach to fatigue with a variational phase-field model: The one-dimensional case. *Engineering fracture mechanics*, 190:53–73.

[11] Carrara, P. and Ambati, M. and Alessi, R. and De Lorenzis, L. 2020. A framework to model the fatigue behavior of brittle materials based on a variational phase-field approach. *Computer Methods in Applied Mechanics and Engineering*, 361:112731.

[12] Zhu, Q.Z. and Shao, J.F. and Kondo, D. 2011. A micromechanics-based thermodynamic formulation of isotropic damage with unilateral and friction effects. *European Journal of Mechanics-A/Solids*, 30(3):316–325.

[13] Zhu, Q.Z. and Zhao, L.Y. and Shao, J.F. 2016. Analytical and numerical analysis of frictional damage in quasi brittle materials. *Journal of the Mechanics and Physics of Solids*, 92:137–163.

[14] Marigo, J.J. and Kazymyrenko, K. 2019. A micromechanical inspired model for the coupled to damage elasto-plastic behavior

of geomaterials under compression. *Mechanics & Industry*, 20(1):105.

[15] Ulloa, J. and Wambacq, J. and Alessi, R. and Degrande, G. and François, S. 2021. Phase-field modeling of fatigue coupled to cyclic plasticity in an energetic formulation. *Computer Methods in Applied Mechanics and Engineering*, 373:113473.

[16] Sarem, M. and Deresse, N.E. and Ulloa, J. and Verstrynge, E. and François, S. 2023. Micromechanics-based variational phase-field modeling of Brazilian splitting tests. *Engineering Fracture Mechanics*, 290:109472.